This article has been accepted for publication in a future issue of this journal, but has not been fully edited. Content may change prior to final publication. Citation information: DOI 10.1109/LCOMM.2020.3039811, IEEE Communications Letters

Robust and Secure Communications in Intelligent Reflecting Surface Assisted NOMA Networks

Zheng Zhang, Lu Lv, *Member, IEEE*, Qingqing Wu, *Member, IEEE*, Hao Deng, and Jian Chen, *Member, IEEE*

***Abstract*—This letter investigates secure transmission in an intelligent reflecting surface (IRS) assisted non-orthogonal multiple access (NOMA) network. Consider a practical eavesdropping scenario with imperfect channel state information of the eavesdropper, we propose a robust beamforming scheme using artificial noise to guarantee secure NOMA transmission with the IRS. A joint transmit beamforming and IRS phase shift optimization problem is formulated to minimize the transmit power. Since the problem is non-convex and challenging to resolve, we develop an effective alternating optimization (AO) algorithm to obtain stationary point solutions. Simulation results validate the security advantage of the robust beamforming scheme and the effectiveness of the AO algorithm.**

***Index Terms*—Intelligent reflecting surface, non-orthogonal multiple access, physical layer security, robust beamforming.**

I. Introduction

Intelligent reflecting surface (IRS) is a promising technology to achieve high energy and spectrum efficiency for future wireless communications [1], [2]. Particularly, IRS can actively create a reconfigurable radio environment to improve the wireless network performance by adaptively adjusting amplitudes and phase shifts of passive reflecting elements [3]. On the other hand, non-orthogonal multiple access (NOMA) improves spectrum efficiency by exploiting the power-domain multiplexing to serve multiple users with the same time-frequency resource block [4], [5]. It is expected that combining IRS with NOMA could further enhance the network performance, since NOMA is more powerful when the differences of the user channel gains are larger, while IRS can proactively reconfigure user channels to achieve this goal [6]–[8].

With the broadcast nature of wireless channels, the private information is vulnerable to eavesdropping. This thus calls for physical layer security (PLS), which utilizes the characteristics of wireless channels to achieve secure communications. Since IRS can smartly change the wireless propagation environment, it can be exploited to benefit PLS by intelligently adjusting the reflection coefficients for signal enhancement at receiver while signal cancellation/mitigation at eavesdropper [9]–[12].

The aforementioned works [9]–[12] only consider PLS for IRS assisted orthogonal multiple access (OMA) networks, while research on PLS for IRS assisted NOMA networks is still missing in the literature. For IRS assisted NOMA with security considerations, resource allocation becomes rather challenging, because: 1) successive interference cancellation (SIC) decoding constraint of NOMA increases the design complexity of the transmission scheme, and 2) the existence of co-channel interference and secrecy constraints lead to sophisticated interference management for IRS's reflection. Furthermore, existing studies [9]–[11] rely on perfect channel state information (CSI) of eavesdropper which, however, may not hold since eavesdropper is passive and may try to hide itself from legitimate nodes [12]. In this case, only imperfect CSI of eavesdropper is available.

Motivated by the above observations, this letter studies secure transmission in an IRS assisted NOMA network with only the imperfect CSI of a multi-antenna eavesdropper. The major contributions are summarized as follows.

- We propose a robust beamforming scheme to secure IRS assisted NOMA transmission, where artificial noise (AN) is exploited to reduce information leakage to eavesdropper while minimizing the effect on reception quality of legitimate users. A joint active and passive beamforming optimization problem is formulated and solved for transmit power minimization.
- To handle the non-convex constraints due to the eavesdropper's imperfect CSI, we introduce equivalent channel/beamforming matrices to simplify the semi-infinite constraints. Furthermore, a sequential rank-one constraint relaxation (SROCR) based alternating optimization (AO) algorithm is proposed to efficiently optimize the IRS reflection coefficients and the transmit power, where effective rank-one solutions are obtained.
- Numerical results verify the security advantage of proposed scheme over two baseline schemes. In particular, it is found that signal power highly depends on quality-of-service (QoS) constraint of legitimate users, while AN power is extremely sensitive to QoS constraint, maximum eavesdropping rate, and interception capability of eavesdropper.

II. System Model and Problem Formulation

We consider an IRS assisted NOMA network, which consists of two single-antenna users (near user U_1 and cell-edge

This work was partially supported by the National Natural Science Foundation of China under Grants 61901313 and 61771366, the Open Research Fund of National Mobile Communications Research Laboratory, Southeast University, under Grant 2020D07, the Natural Science Basic Research Plan of Shaanxi Province under Grant 2020JQ-306, the China Postdoctoral Science Foundation under Grants BX20190264 and 2019M650258, the Natural Science Foundation of Henan under Grant 202300410094, and the Key Scientific Research Projects of Higher Education Institutions in Henan Province under Grant 20A510002. The associate editor coordinating the review of this letter and approving it for publication was N. I. Miridakis. *(Corresponding author: Jian Chen.)*

Zheng Zhang and Jian Chen are with the State Key Laboratory of Integrated Services Networks, Xidian University, Xi'an 710071, China (e-mail: zzhang_688@stu.xidian.edu.cn; jianchen@mail.xidian.edu.cn).

Lu Lv is with the State Key Laboratory of Integrated Services Networks, Xidian University, Xi'an 710071, China, and also with the National Mobile Communications Research Laboratory, Southeast University, Nanjing 210096, China (e-mail: lulv@xidian.edu.cn).

Qingqing Wu is with the State Key Laboratory of Internet of Things for Smart City, University of Macau, Macau 999078, China (e-mail: qingqingwu@um.edu.mo).

Hao Deng is with the School of Physics and Electronics, Henan University, Kaifeng 475001, China (e-mail: gavind@163.com).

user U_2), an N_t-antenna base station (BS), an IRS, and an N_e-antenna eavesdropper (E) near BS. This is a typical scenario in cellular networks, since the legitimate users usually have limited reception capacities, while the BS and eavesdropper have the strong transmit/reception abilities. We further assume that there is no direct link between the BS and U_2 due to the existence of obstacles and the severe path loss over long distances, which thus motivates the deployment of IRS to establish a reliable communication link between them. Moreover, $N_\mathrm{t} > N_\mathrm{e}$ should be satisfied in order to prevent eavesdropper from eliminating the AN by using the null-space receive beamforming [14]. As U_1 and E locate close to the BS, they have direct links to the BS. In each transmission, the BS utilizes NOMA to simultaneously transmit superimposed signals and AN, where AN is used to confuse E[1]. The IRS is connected to a smart controller and has M passive reflecting elements, each of which can change its amplitude and phase independently to improve the reception quality of both U_1 and U_2 while degrading the interception capability of E.

The received signals at U_1, U_2 and E are given by

$$y_1 = (\mathbf{h}_{\mathrm{I},1}^H \mathbf{\Theta} \mathbf{H}_{\mathrm{B,I}} + \mathbf{h}_{\mathrm{B},1}^H)(\textstyle\sum_{i=1}^{2} \mathbf{w}_i s_i + \mathbf{s}_{\mathrm{AN}}) + n_1, \quad (1)$$

$$y_2 = (\mathbf{h}_{\mathrm{I},2}^H \mathbf{\Theta} \mathbf{H}_{\mathrm{B,I}})(\textstyle\sum_{i=1}^{2} \mathbf{w}_i s_i + \mathbf{s}_{\mathrm{AN}}) + n_2, \quad (2)$$

$$\mathbf{y}_\mathrm{e} = (\mathbf{G}_{\mathrm{I,e}}^H \mathbf{\Theta} \mathbf{H}_{\mathrm{B,I}} + \mathbf{G}_{\mathrm{B,e}}^H)(\textstyle\sum_{i=1}^{2} \mathbf{w}_i s_i + \mathbf{s}_{\mathrm{AN}}) + \mathbf{n}_\mathrm{e}, \quad (3)$$

where $\mathbf{h}_{\mathrm{I},i} \in \mathbb{C}^{M\times 1}$ $(1 \leqslant i \leqslant 2)$, $\mathbf{h}_{\mathrm{B},1} \in \mathbb{C}^{N_\mathrm{t}\times 1}$, $\mathbf{H}_{\mathrm{B,I}} \in \mathbb{C}^{M\times N_\mathrm{t}}$ $\mathbf{G}_{\mathrm{B,e}} \in \mathbb{C}^{N_\mathrm{t}\times N_\mathrm{e}}$, and $\mathbf{G}_{\mathrm{I,e}} \in \mathbb{C}^{M\times N_\mathrm{e}}$ denote the channel vectors/matrixes of transmission links IRS-U_i $(1 \leqslant i \leqslant 2)$, BS-$\mathrm{U}_1$, BS-IRS, BS-E, and IRS-E, respectively. s_i denotes the signal of U_i with the corresponding beamfoming vector $\mathbf{w}_i \in \mathbb{C}^{N_\mathrm{t}\times 1}$, which satisfies $\mathbb{E}\{|s_i|^2\} = 1$. $\mathbf{s}_{\mathrm{AN}} \in \mathbb{C}^{N_\mathrm{t}\times 1}$ denotes the AN vector following circularly symmetric complex Gaussian distribution with zero mean and covariance matrix $\mathbf{W}_{\mathrm{AN}}$. $n_1, n_2 \sim \mathcal{CN}(0, \sigma_\mathrm{n}^2)$ and $\mathbf{n}_\mathrm{e} \sim \mathcal{CN}(\mathbf{0}, \sigma_\mathrm{n}^2 \mathbf{I}_{N_\mathrm{e}})$ are the additive white Gaussian noises (AWGNs) at users and E, respectively. To explore the fundamental performance limit of the considered network, we assume that the reflection coefficients of the IRS can be arbitrary amplitudes and phase shift values, i.e., $\mathbf{\Theta} = \mathrm{diag}(\beta_1 e^{j\theta_1}, \ldots, \beta_M e^{j\theta_M}) \in \mathbb{C}^{M\times M}$, where $\beta_m \in [0, 1]$ and $\theta_m \in [0, 2\pi]$ for $1 \leqslant m \leqslant M$.

As for U_2's signal decoding, s_2 is detected firstly by treating s_1 as noise at each receiver, then U_1 will remove s_2 from the detect result and decoding s_1 without inter-user interference. Accordingly, the achievable rates for U_1 to decode s_1 and s_2 are given, respectively, by

$$R_{1,1} = \log_2\left(1 + \frac{|\mathbf{h}_1^H \mathbf{w}_1|^2}{\mathrm{Tr}(\mathbf{h}_1^H \mathbf{h}_1 \mathbf{W}_{\mathrm{AN}}) + \sigma_\mathrm{n}^2}\right), \quad (4)$$

$$R_{1,2} = \log_2\left(1 + \frac{|\mathbf{h}_1^H \mathbf{w}_2|^2}{|\mathbf{h}_1^H \mathbf{w}_1|^2 + \mathrm{Tr}(\mathbf{h}_1^H \mathbf{h}_1 \mathbf{W}_{\mathrm{AN}}) + \sigma_\mathrm{n}^2}\right). \quad (5)$$

[1]Our work can be expanded into multi-carrier or multiuser NOMA. For multi-carrier NOMA, a near user and a cell-edge user are associated with one subcarrier to perform NOMA transmission. In multiuser NOMA, we can adopt the matching theory to divide legitimate users into user pairs for NOMA transmission in time-selectivity manner. However, the multiple users will increase the transmit power consumption, and the subcarrier-users assignment and user matching challenge the reflection optimization and algorithm design.

While U_2 directly decodes s_2 by treating s_1 as noise yielding the achievable rate as

$$R_{2,2} = \log_2\left(1 + \frac{|\mathbf{h}_2^H \mathbf{w}_2|^2}{|\mathbf{h}_2^H \mathbf{w}_1|^2 + \mathrm{Tr}(\mathbf{h}_2^H \mathbf{h}_2 \mathbf{W}_{\mathrm{AN}}) + \sigma_\mathrm{n}^2}\right). \quad (6)$$

We adopt a worst-case assumption in PLS, namely, E has strong multiuser detection capacity and can remove inter-user interference in NOMA secrecy [14]. Thus, the eavesdropping rates at E for s_1 and s_2 are shown as

$$R_{\mathrm{e},1} = \log_2 \det(\mathbf{I}_{N_\mathrm{e}} + \mathbf{Q}^{-1} \mathbf{G}_\mathrm{e}^H \mathbf{w}_1 \mathbf{w}_1^H \mathbf{G}_\mathrm{e}), \quad (7)$$

$$R_{\mathrm{e},2} = \log_2 \det(\mathbf{I}_{N_\mathrm{e}} + \mathbf{Q}^{-1} \mathbf{G}_\mathrm{e}^H \mathbf{w}_2 \mathbf{w}_2^H \mathbf{G}_\mathrm{e}), \quad (8)$$

where $\mathbf{G}_\mathrm{e}^H = \mathbf{G}_{\mathrm{I,e}}^H \mathbf{\Theta} \mathbf{H}_{\mathrm{B,I}} + \mathbf{G}_{\mathrm{B,e}}^H$ and $\mathbf{Q} = \mathbf{G}_\mathrm{e}^H \mathbf{W}_{\mathrm{AN}} \mathbf{G}_\mathrm{e} + \sigma_\mathrm{n}^2 \mathbf{I}_{N_\mathrm{e}}$.

A. Imperfect Channel State Information

In this paper, we assume that the CSI of legitimate users is perfectly available to BS, which can be realized by the channel estimation method in [16] [17]. While the perfect CSI of E is difficult to obtain since E usually belongs to third party networks and can wiretap legitimate communications with keeping silent. In this case, the BS is capable of utilizing the inadvertent local oscillator power leakage from the radio frequency front-end of the E to estimate CSI, which, however, is inexact and outdated [12]. To describe E's imperfect CSI, we adopt the ellipsoidal bounded channel uncertainty model as follows

$$\Delta\mathbf{G}_{\mathrm{I,e}} = \mathbf{G}_{\mathrm{I,e}} - \hat{\mathbf{G}}_{\mathrm{I,e}},\ \Delta\mathbf{G}_{\mathrm{B,e}} = \mathbf{G}_{\mathrm{B,e}} - \hat{\mathbf{G}}_{\mathrm{B,e}}, \quad (9)$$

$$\Omega_\mathrm{e} = \{\|\Delta\mathbf{G}_{\mathrm{I,e}}\|_F \leqslant \varepsilon_{\mathrm{I,e}}, \|\Delta\mathbf{G}_{\mathrm{B,e}}\|_F \leqslant \varepsilon_{\mathrm{B,e}}\}, \quad (10)$$

where $\hat{\mathbf{G}}_{\mathrm{I,e}}$ and $\hat{\mathbf{G}}_{\mathrm{B,e}}$ represent the estimated channels of $\mathbf{G}_{\mathrm{I,e}}$ and $\mathbf{G}_{\mathrm{B,e}}$, while $\varepsilon_{\mathrm{I,e}} > 0$ and $\varepsilon_{\mathrm{B,e}} > 0$ denote the sizes of the uncertainty regions of channel estimation errors $\Delta\mathbf{G}_{\mathrm{I,e}}$ and $\Delta\mathbf{G}_{\mathrm{B,e}}$, respectively, and $\|\cdot\|_F$ is the Frobenius norm.

B. Problem Formulation

To guarantee robust and secure transmission, a worst-case optimization problem is investigated. Specifically, we aim at minimizing the total transmit power by joint active and passive beamforming, subject to the minimum QoS constraints at users and the maximum eavesdropping rates at E. The optimization problem is formulated as follows

$$\min_{\mathbf{w}_i, \mathbf{W}_{\mathrm{AN}}, \mathbf{\Theta}} \quad \textstyle\sum_{i=1}^{2} \|\mathbf{w}_i\|^2 + \mathrm{Tr}(\mathbf{W}_{\mathrm{AN}}) \quad (11a)$$

$$\text{s.t.} \quad \theta_m \in [0, 2\pi],\ \beta_m \in [0, 1],\ \forall m, \quad (11b)$$

$$R_{i,i} \geqslant R_{\mathrm{Q}_i},\ \forall i, \quad (11c)$$

$$\max_{\Omega_\mathrm{e}} R_{\mathrm{e},i} \leqslant R_\mathrm{M},\ \forall i, \quad (11d)$$

$$R_{1,2} \geqslant R_{2,2}, \quad (11e)$$

$$|\mathbf{h}_i^H \mathbf{w}_2|^2 \geqslant |\mathbf{h}_i^H \mathbf{w}_1|^2,\ \forall i, \quad (11f)$$

where R_{Q_i} denotes the QoS requirement of U_i and R_M denotes the maximum eavesdropping rate at E. Constraint (11b) represents the IRS amplitudes/phase shifts requirements. Constraints (11c) and (11d) guarantee a positive rate gap between legitimate transmission rates and eavesdropping rates. The inequality in (11e) insures a successful SIC decoding at U_1. Constraint (11f) determines the SIC decoding order of the NOMA users. Problem (11a) is intractable to solve due to the semi-infinite constraints (11d) and coupled variables $\mathbf{\Theta}$ and $\mathbf{w}_i$. Next, we develop an efficient AO algorithm to solve it.

III. Robust Beamforming Design

This section proposes an AO algorithm to efficiently solve problem (11a). Specifically, we first introduce equivalent channel/beamforming matrices to transform the semi-infinite constraints into a tractable form, which can be directly tackled by S-procedure. Then, to handle the non-convex constraints caused by the coupled variables, we optimize the active and passive beamforming in an alternative manner.

A. Transformation of Semi-Infinite Constraint

According to [12, Prop. 1], we first rewrite (11d) into the following form:

$$\mathbf{G}_{\rm e}^H\mathbf{W}_i'\mathbf{G}_{\rm e}+\sigma_{\rm n}^2(2^{R_{\rm M}}-1)\mathbf{I}_{N_{\rm e}}\succeq\mathbf{0},\ \forall i, \tag{12}$$

where $\mathbf{W}_i'=(2^{R_{\rm M}}-1)\mathbf{W}_{\rm AN}-\mathbf{W}_i$ and $\mathbf{W}_i=\mathbf{w}_i\mathbf{w}_i^H$ for $1\leqslant i\leqslant 2$, which should satisfy constraints $\mathbf{W}_i\succeq\mathbf{0}$ and $\text{rank}(\mathbf{W}_i)=1$. Then, substituting (9) into (12), (11d) can be further expressed as the following quadratic form:

$$\begin{aligned}&(\hat{\mathbf{G}}_{\rm I,e}^H\boldsymbol{\Theta}\mathbf{H}_{\rm B,I}+\hat{\mathbf{G}}_{\rm B,e}^H)\mathbf{W}_i'(\hat{\mathbf{G}}_{\rm I,e}^H\boldsymbol{\Theta}\mathbf{H}_{\rm B,I}+\hat{\mathbf{G}}_{\rm B,e}^H)^H+\\&(\Delta\mathbf{G}_{\rm I,e}^H\boldsymbol{\Theta}\mathbf{H}_{\rm B,I}+\Delta\mathbf{G}_{\rm B,e}^H)\mathbf{W}_i'(\hat{\mathbf{G}}_{\rm I,e}^H\boldsymbol{\Theta}\mathbf{H}_{\rm B,I}+\hat{\mathbf{G}}_{\rm B,e}^H)^H+\\&(\hat{\mathbf{G}}_{\rm I,e}^H\boldsymbol{\Theta}\mathbf{H}_{\rm B,I}+\hat{\mathbf{G}}_{\rm B,e}^H)\mathbf{W}_i'(\Delta\mathbf{G}_{\rm I,e}^H\boldsymbol{\Theta}\mathbf{H}_{\rm B,I}+\Delta\mathbf{G}_{\rm B,e}^H)^H+\\&(\Delta\mathbf{G}_{\rm I,e}^H\boldsymbol{\Theta}\mathbf{H}_{\rm B,I}+\Delta\mathbf{G}_{\rm B,e}^H)\mathbf{W}_i'(\Delta\mathbf{G}_{\rm I,e}^H\boldsymbol{\Theta}\mathbf{H}_{\rm B,I}+\Delta\mathbf{G}_{\rm B,e}^H)^H+\\&\sigma_{\rm n}^2(2^{R_{\rm M}}-1)\mathbf{I}_{N_{\rm e}}\succeq\mathbf{0},\ \forall i.\end{aligned} \tag{13}$$

To handle (13), we define the equivalent channel estimation error and estimated channel matrices of E as

$$\Delta\mathbf{X}^H=[\Delta\mathbf{G}_{\rm I,e}^H,\Delta\mathbf{G}_{\rm B,e}^H],\ \hat{\mathbf{X}}^H=[\hat{\mathbf{G}}_{\rm I,e}^H,\hat{\mathbf{G}}_{\rm B,e}^H]. \tag{14}$$

Furthermore, a joint beamforming matrix is defined as

$$\mathbf{V}_i=\begin{bmatrix}\boldsymbol{\Theta}\mathbf{H}_{\rm B,I}\mathbf{W}_i'\mathbf{H}_{\rm B,I}^H\boldsymbol{\Theta}^H & \boldsymbol{\Theta}\mathbf{H}_{\rm B,I}\mathbf{W}_i'\\ \mathbf{W}_i'\mathbf{H}_{\rm B,I}^H\boldsymbol{\Theta}^H & \mathbf{W}_i'\end{bmatrix},\ \forall i. \tag{15}$$

Thus, combining (13), (14) and (15), we obtain

$$\begin{aligned}&\Delta\mathbf{X}^H\mathbf{V}_i\Delta\mathbf{X}+\Delta\mathbf{X}^H\mathbf{V}_i\hat{\mathbf{X}}+\hat{\mathbf{X}}^H\mathbf{V}_i\Delta\mathbf{X}+\hat{\mathbf{X}}^H\mathbf{V}_i\hat{\mathbf{X}}+\sigma_{\rm n}^2\mathbf{I}_{N_{\rm e}}\\&(2^{R_{\rm M}}-1)\succeq\mathbf{0},\Delta\mathbf{X}\in\{\mathbf{Y}|\text{Tr}(\varepsilon_{\rm e}^{-2}\mathbf{Y}\mathbf{Y}^H)\leqslant 1\},\forall i,\end{aligned} \tag{16}$$

where $\varepsilon_{\rm e}=\varepsilon_{\rm B,e}+\varepsilon_{\rm I,e}$. Afterwards, by adopting S-procedure [15], the infinite inequality (16) can be transformed into a finite linear matrix inequality (LMI) as

$$\begin{bmatrix}\hat{\mathbf{X}}^H\mathbf{V}_i\hat{\mathbf{X}}+(\sigma_{\rm n}^2\gamma_{\rm M}-\tau_i)\mathbf{I}_{N_{\rm e}} & \hat{\mathbf{X}}^H\mathbf{V}_i\\ \mathbf{V}_i\hat{\mathbf{X}} & \mathbf{V}_i+\tau_i\varepsilon_{\rm e}^{-2}\mathbf{I}_M\end{bmatrix}\succeq\mathbf{0},\forall i, \tag{17}$$

where $\gamma_{\rm M}=2^{R_{\rm M}}-1$, and $\tau_i>0$ denotes an auxiliary variable introduced by S-procedure.

B. Active Beamforming Optimization

By fixing $\boldsymbol{\Theta}$, the optimization problem becomes:

$$\min_{\mathbf{W}_i,\mathbf{W}_{\rm AN},\tau_i}\ \sum\nolimits_{i=1}^2\text{Tr}(\mathbf{W}_i)+\text{Tr}(\mathbf{W}_{\rm AN}) \tag{18a}$$
$$\text{s.t.}\quad (11\text{c}),(11\text{e}),(11\text{f}),(17), \tag{18b}$$
$$\mathbf{W}_i\succeq\mathbf{0},\ \forall i, \tag{18c}$$
$$\text{rank}(\mathbf{W}_i)=1,\ \forall i. \tag{18d}$$

For notation brevity, we denote $\mathbf{H}_{\rm W,1}=\mathbf{h}_1\mathbf{h}_1^H$ and $\mathbf{H}_{\rm W,2}=\mathbf{h}_2\mathbf{h}_2^H$. Thus, constraints (11c) and (11f) can be rewritten as

$$\text{Tr}(\mathbf{H}_{\rm W,1}\mathbf{W}_1)\geqslant\gamma_{\rm Q}(\text{Tr}(\mathbf{H}_{\rm W,1}\mathbf{W}_{\rm AN})+\sigma_{\rm n}^2), \tag{19a}$$
$$\text{Tr}(\mathbf{H}_{\rm W,2}\mathbf{W}_2)\geqslant\gamma_{\rm Q}(\text{Tr}(\mathbf{H}_{\rm W,2}\mathbf{W}_{\rm AN})+\text{Tr}(\mathbf{H}_{\rm W,2}\mathbf{W}_1)+\sigma_{\rm n}^2), \tag{19b}$$
$$\text{Tr}(\mathbf{H}_{{\rm W},i}\mathbf{W}_2)\geqslant\text{Tr}(\mathbf{H}_{{\rm W},i}\mathbf{W}_1),\forall i, \tag{19c}$$

where $\gamma_{\rm Q}=2^{R_{\rm Q}}-1$. For constraint (11e), we introduce a slack variable $\gamma_t>0$, which satisfies

$$\text{Tr}(\mathbf{H}_{\rm W,1}\mathbf{W}_2)\geqslant(\text{Tr}(\mathbf{H}_{\rm W,1}\mathbf{W}_{\rm AN})+\text{Tr}(\mathbf{H}_{\rm W,1}\mathbf{W}_1)+\sigma_{\rm n}^2)\gamma_t, \tag{20a}$$
$$\text{Tr}(\mathbf{H}_{\rm W,2}\mathbf{W}_2)\leqslant(\text{Tr}(\mathbf{H}_{\rm W,2}\mathbf{W}_{\rm AN})+\text{Tr}(\mathbf{H}_{\rm W,2}\mathbf{W}_1)+\sigma_{\rm n}^2)\gamma_t. \tag{20b}$$

In (20a), it is not difficult to see that the term of $\text{Tr}(\mathbf{H}_{\rm W,1}\mathbf{W}_{\rm AN})+\text{Tr}(\mathbf{H}_{\rm W,1}\mathbf{W}_1)+\sigma_{\rm n}^2$ is nonnegative. Thus, we apply the arithmetic geometry mean (AGM) inequality to approximate (20a) by

$$\begin{aligned}2\text{Tr}(\mathbf{H}_{\rm W,1}\mathbf{W}_2)\geqslant&((\text{Tr}(\mathbf{H}_{\rm W,1}\mathbf{W}_{\rm AN})+\text{Tr}(\mathbf{H}_{\rm W,1}\mathbf{W}_1)+\sigma_{\rm n}^2)\varpi)^2\\&+(\gamma_t/\varpi)^2,\end{aligned} \tag{21}$$

where the equality holds if and only if when $\varpi=\sqrt{\frac{\gamma_t}{\text{Tr}(\mathbf{H}_{\rm W,1}\mathbf{W}_{\rm AN})+\text{Tr}(\mathbf{H}_{\rm W,1}\mathbf{W}_1)+\sigma_{\rm n}^2}}$. In (20b), we introduce another slack variable ν, which satisfies

$$\text{Tr}(\mathbf{H}_{\rm W,2}\mathbf{W}_2)\leqslant 2\tilde{\nu}\nu-\tilde{\nu}^2, \tag{22}$$

where the right-hand side of (22) is the Taylor series expansion of the quadratic function ν^2, and $\tilde{\nu}$ denotes the reference point of ν. Then, (20b) can be reshaped as

$$\begin{bmatrix}\text{Tr}(\mathbf{H}_{\rm W,2}\mathbf{W}_{\rm AN})+\text{Tr}(\mathbf{H}_{\rm W,2}\mathbf{W}_1)+\sigma_{\rm n}^2 & \nu\\ \nu & \gamma_t\end{bmatrix}\succeq\mathbf{0}. \tag{23}$$

To deal with with the non-convex rank-one constraints (18d), we consider the SROCR method [13] to obtain rank-one solutions of problem (18a), which is described as follows. The rank-one constraint $\text{rank}(\mathbf{W}_i^{(n)})=1$ at the *n*th iteration is replaced by the linear constraint

$$\mathbf{w}_i^{\text{eig-max},(n-1)}\mathbf{W}_i^{(n)}\mathbf{w}_i^{\text{eig-max},(n-1)}\geqslant w_i^{(n-1)}\text{Tr}(\mathbf{W}_i^{(n)}). \tag{24}$$

In (24), $w_i^{(n-1)}\in[0,1]$ denotes the trace ratio parameter of $\mathbf{W}_i$ at the $(n-1)$th iteration, which gradually increases from 0 to 1. $\mathbf{w}_i^{\text{eig-max},(n-1)}\in\mathbb{C}^{N_{\rm t}\times 1}$ denotes the eigenvector of the largest eigenvalue of $\mathbf{W}_i^{(n-1)}$ with the parameter $w_i^{(n-1)}$. The iterative convex program (ICP) at the *n*th iteration is given by

$$\min_{\mathbf{W}_i,\mathbf{W}_{\rm AN},\tau_i,\gamma_t,\nu}\ \sum\nolimits_{i=1}^2\text{Tr}(\mathbf{W}_i)+\text{Tr}(\mathbf{W}_{\rm AN}) \tag{25a}$$
$$\text{s.t.}\quad (17),(18\text{c}),(19\text{a})-(19\text{c}),(21),\ (22),(23),(24). \tag{25b}$$

The ICP can be solved efficiently by using the CVX toolbox, and the iterative algorithm for problem (25a) is summarized in **Algorithm-1**, where $P_{\rm t}$ denotes the total transmit power at BS and δ denotes the convergence accuracy.

C. Passive Beamforming Optimization

With the given $\mathbf{W}_i$ and $\mathbf{W}_{\rm AN}$, we can denote $\mathbf{u}_0=[\beta_1e^{j\theta_1},\ldots,\beta_Me^{j\theta_M}]^H$, $\mathbf{u}=[\mathbf{u}_0;1]$, $\mathbf{U}\triangleq\mathbf{u}\mathbf{u}^H$, $\mathbf{H}_{\rm U,1}=[\text{diag}(\mathbf{h}_{\rm I,1}^H)\mathbf{H}_{\rm B,I};\mathbf{h}_{\rm B,1}^H]$ and $\mathbf{H}_{\rm U,2}=[\text{diag}(\mathbf{h}_{\rm I,2}^H)\mathbf{H}_{\rm B,I};\mathbf{0}]$. Therefore, the constraint (19a), (19b) and (19c) can be transformed into

$$\text{Tr}(\mathbf{U}_{1,1}')\geqslant\gamma_{\rm Q}(\text{Tr}(\mathbf{U}_{\rm AN,1}')+\sigma_{\rm n}^2), \tag{26a}$$
$$\text{Tr}(\mathbf{U}_{2,2}')\geqslant\gamma_{\rm Q}(\text{Tr}(\mathbf{U}_{\rm AN,2}')+\text{Tr}(\mathbf{U}_{1,2}')+\sigma_{\rm n}^2), \tag{26b}$$

Algorithm-1: Iterative Algorithm for Solving Problem (18a)

1: **Initialization**: set $n = 1$ and initialize $\varpi^{(0)}$, $\tilde{\nu}^{(0)}$, $w_i^{(0)}$, $\mathbf{w}_i^{\text{eig-max},(0)}$;
2: **Repeat:**
3: **If** the ICP (25a) is feasible, solve the problem, define $\epsilon^{(n)} = \epsilon^{(n-1)}$ and update $\varpi^{(n)}$ and $\tilde{\nu}^{(n)}$;
4: **Else**: define $\epsilon^{(n)} = \frac{1}{2}\epsilon^{(n-1)}$;
5: Update $w_i^{(n)} = \min(1, \frac{\lambda_{\max}(\mathbf{W}_i^{(n)})}{\mathrm{Tr}(\mathbf{W}_i^{(n)})} + \epsilon^{(n)})$;
6: $n = n + 1$;
7: **Until:** $w_i^{(n)} = 1$ and $|P_t^{(n)} - P_t^{(n-1)}| \leqslant \delta$.

$$\mathrm{Tr}(\mathbf{U}'_{2,i}) \geqslant \mathrm{Tr}(\mathbf{U}'_{1,i}), \forall i, \tag{26c}$$

where $\mathbf{U}'_{\varrho,i} = \mathbf{H}_{\mathrm{U},i}\mathbf{W}_\varrho\mathbf{H}_{\mathrm{U},i}^H\mathbf{U}$ for $\varrho \in \{1, 2, \mathrm{AN}\}$ and $i \in \{1, 2\}$. Similarly, the constraints (21), (22) and (23) can be rewritten as

$$\begin{aligned} 2\mathrm{Tr}(\mathbf{U}'_{2,1}) \geqslant &((\mathrm{Tr}(\mathbf{U}'_{\mathrm{AN},1}) + \mathrm{Tr}(\mathbf{U}'_{1,1}) + \sigma_{\mathrm{n}}^2)\varpi)^2 \\ &+ (\gamma_t/\varpi)^2, \end{aligned} \tag{27}$$

$$\mathrm{Tr}(\mathbf{U}'_{2,2}) \leqslant 2\tilde{\nu}\nu - \tilde{\nu}^2, \tag{28}$$

$$\begin{bmatrix} \mathrm{Tr}(\mathbf{U}'_{\mathrm{AN},2}) + \mathrm{Tr}(\mathbf{U}'_{1,2}) + \sigma_{\mathrm{n}}^2 & \nu \\ \nu & \gamma_t \end{bmatrix} \succeq \mathbf{0}. \tag{29}$$

For the non-convex term $\mathbf{V}_i$ in (15), we utilize the singular value decomposition (SVD) to transform $\mathbf{H}_{\mathrm{B,I}}\mathbf{W}'_i\mathbf{H}_{\mathrm{B,I}}^H$ into $\sum_p \mathbf{s}_{i,p}\mathbf{d}_{i,p}$, which represents $\mathbf{\Theta}\mathbf{H}_{\mathrm{B,I}}\mathbf{W}'_i\mathbf{H}_{\mathrm{B,I}}^H\mathbf{\Theta}^H$ in an equivalent form $\sum_p \mathrm{diag}(\mathbf{s}_{i,p})\bar{\mathbf{u}}_0\bar{\mathbf{u}}_0^H\mathrm{diag}(\mathbf{d}_{i,p})$. Based on the properties of matrix, we have the following equation:

$$\mathrm{diag}(\mathbf{s}_{i,p})\bar{\mathbf{u}}_0\bar{\mathbf{u}}_0^H\mathrm{diag}(\mathbf{d}_{i,p}) = \mathbf{S}_{i,p}\bar{\mathbf{u}}\bar{\mathbf{u}}^H\mathbf{D}_{i,p}, \ \forall i, p, \tag{30}$$

where $\mathbf{S}_{i,p} = [\mathrm{diag}(\mathbf{s}_{i,p}), \mathbf{0}]$ and $\mathbf{D}_{i,p} = \begin{bmatrix}\mathrm{diag}(\mathbf{d}_{i,p}) \\ \mathbf{0}\end{bmatrix}$. Moreover, when the condition of $\mathrm{rank}(\mathbf{U}) = 1$ holds, $\mathbf{\Theta}$ can be denoted by $\mathrm{diag}(\mathbf{U}_{N+1,1:N})$ equivalently, where $\mathbf{U}_{N+1,1:N}$ equals to $[\mathbf{U}_{N+1,1}, \ldots, \mathbf{U}_{N+1,N}]$. Therefore, non-convex term $\mathbf{V}_i$ can be rewritten as $\begin{bmatrix} \sum_p \mathbf{S}_{i,p}\mathbf{U}^T\mathbf{D}_{i,p} & \mathrm{diag}(\mathbf{U}_{N+1,1:N})\mathbf{H}_{\mathrm{B,I}}\mathbf{W}'_i \\ \mathbf{W}'_i\mathbf{H}_{\mathrm{B,I}}^H\mathrm{diag}(\mathbf{U}_{N+1,1:N})^H & \mathbf{W}'_i \end{bmatrix}$.

Consequently, the feasibility program can be formulated as follows

$$\begin{aligned} &\text{find} \quad \mathbf{U} && \text{(31a)} \\ &\text{s.t.} \quad (17), (26a)-(26c), (27), (28), (29), (30), && \text{(31b)} \\ &\qquad \mathbf{U} \succeq \mathbf{0}, && \text{(31c)} \\ &\qquad \mathbf{U}_{m,m} \leqslant 1, 1 \leqslant m \leqslant M, \mathbf{U}_{M+1,M+1} = 1, && \text{(31d)} \\ &\qquad \mathrm{rank}(\mathbf{U}) = 1. && \text{(31e)} \end{aligned}$$

However, problem (31a) is still non-convex due to the rank-one constraint (31e). Similarly, we use the SROCR method to tackle this problem. The relaxed rank-one constraint at the nth iteration is given by

$$\mathbf{u}^{\text{eig-max},(n-1)}\mathbf{U}^{(n)}\mathbf{u}^{\text{eig-max},(n-1)} \geqslant u^{(n-1)}\mathrm{Tr}(\mathbf{U}^{(n)}). \tag{32}$$

Hence, we have the iterative convex feasibility program (ICFP) at the nth iteration as

$$\begin{aligned} &\text{find} \quad \mathbf{U} && \text{(33a)} \\ &\text{s.t.} \quad (31b)-(31d), (32). && \text{(33b)} \end{aligned}$$

The iterative algorithm to solve problem (33a) is similar to **Algorithm-1** and is thus omitted for brevity.

The AO algorithm is summarized in **Algorithm-2**[2], where for the sub-problem (25a), the overall complexity with interior-point method is $\mathcal{O}\big(l_{\mathrm{a}}(3N_{\mathrm{t}}^2 + 3)^{3.5}\big)$ [18]. $3N_{\mathrm{t}}^2 + 3$ denotes the number of the variables, and l_{a} is the iteration number for solving ICP (25a). Similarly, the computational complexity for solving ICFP (33a) is $\mathcal{O}\big(l_{\mathrm{p}}(M+1)^7\big)$. Therefore, the overall complexity of the AO algorithm is $\mathcal{O}\big(l_{\mathrm{AO}}(l_{\mathrm{a}}(3N_{\mathrm{t}}^2 + 3)^{3.5} + l_{\mathrm{p}}(M+1)^7)\big)$, where l_{AO} represents the alternating iteration numbers.

Algorithm-2: AO Algorithm for Solving Problem (11a)

1: **Initialization**: Set $k = 1$, and initialize $\varpi^{(0)}$, $\tilde{\nu}^{(0)}$, $\mathbf{\Theta}^{(0)}$, $w_i^{(0)}$, $\mathbf{w}_i^{\text{eig-max},(0)}$, $u^{(0)}$ and $\mathbf{u}^{\text{eig-max},(0)}$;
2: **Repeat**:
3: Solve ICP (25a) with fixed $\mathbf{\Theta}^{(k-1)}$;
4: Solve ICFP (33a) with fixed $\mathbf{W}_i^{(k)}$ and $\mathbf{W}_{\mathrm{AN}}^{(k)}$;
5: $k = k + 1$;
6: **Until:** $|P_t^{(k)} - P_t^{(k-1)}| \leqslant \delta$.

IV. Numerical Results

In this section, we present numerical results to verify the performance of the proposed solution. The locations of all nodes are shown in Fig. 1, and since IRS typically supports nearby users with low speed, the line-of-sight (Los) links have the significant impacts on the performance of transmissions. Thus here, we assume all the channels follow Rician fading, i.e., $\mathbf{h} = \sqrt{L_0 d^{-\alpha}}(\sqrt{\frac{\kappa}{1+\kappa}}\mathbf{h}_{\mathrm{Los}} + \sqrt{\frac{1}{1+\kappa}}\mathbf{h}_{\mathrm{NLos}})$, where $\mathbf{h} \in \{\mathbf{h}_{\mathrm{I},i}, \mathbf{h}_{\mathrm{B},1}, \mathbf{H}_{\mathrm{B,I}}, \mathbf{G}_{\mathrm{B,e}}, \mathbf{G}_{\mathrm{I,e}}\}$. $\mathbf{h}_{\mathrm{Los}}$ and $\mathbf{h}_{\mathrm{NLos}}$ respectively denote the Los and non-line-of-sight (NLos) small-scale fading components. L_0 represents the path loss at the reference distance of 1 meter, κ represents the Rician factor, while d and α denote the transmission distance and path-loss exponents, respectively. The simulation parameters are set as $L_0 = -30$dB, $\sigma_{\mathrm{n}}^2 = -75$dBm, $\kappa_{\mathrm{Los}} = 5$, $\kappa_{\mathrm{NLos}} = 0$, $\alpha_{\mathrm{B},\varsigma} = 3.5$, $\alpha_{\mathrm{B,I}} = 2.2$, and $\alpha_{\mathrm{I},\varsigma} = 2.8$ for $\varsigma \in \{1, 2, \mathrm{e}\}$ [7] [12]. We adopt the normalized channel estimation error uncertainty for simulations, defined as $\xi_{\mathrm{n}} = \frac{\varepsilon_{\mathrm{e}}}{\|\hat{\mathbf{X}}\|_F}$. The convergence accuracy δ is set as 0.1, and each point is averaged over 100 trials.

Fig. 2 illustrates the transmit power of BS versus different QoS requirement of legitimate users. It is observed from the figure that the transmit power of BS monotonically decreases with a increase in QoS rate of U_1 under the fixed sum QoS rate constraint. This be explained by the fact that the same QoS requirement of U_2 consumes more power due to the severe path loss over long distances, Thus, the fairness QoS scheme (i.e., $R_{\mathrm{Q}_1} = R_{\mathrm{Q}_2}$) will require more power compared to the case of $R_{\mathrm{Q}_1} > R_{\mathrm{Q}_2}$. Meanwhile, the increase of the sum QoS rate also requires more transmit power for ensuring legitimate transmissions. Moreover, a larger number of transmit antennas can offer the extra spatial degrees of freedom, which leads to a decrease in the power consumption.

Fig. 3 compares the transmit power achieved by AO algorithm with two baseline schemes, i.e., random phase (RP)

[2] All the iteration parameters are initialized as 1, and the initial eigenvectors are set as $[1, \ldots, 1]^T$. While the phase shift $\theta_m^{(0)}$ are randomly generated in the uniformly distributed interval $[0, 2\pi)$, with the amplitude $\beta_m^{(0)} = 1$.

This article has been accepted for publication in a future issue of this journal, but has not been fully edited. Content may change prior to final publication. Citation information: DOI 10.1109/LCOMM.2020.3039811, IEEE Communications Letters

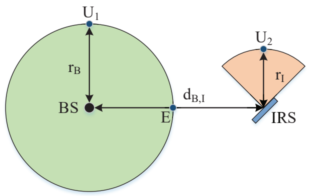

Fig. 1. Simulation setup with $d_{B,I} = 50$m, $r_B = 10$m, and $r_I = 5$m.

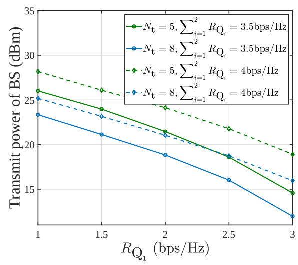

Fig. 2. Transmit power of BS versus the QoS rate of U_1 with $\xi_n = 0.05$, $N_e = 2$, $M = 10$, and $R_M = 0.5$bps/Hz.

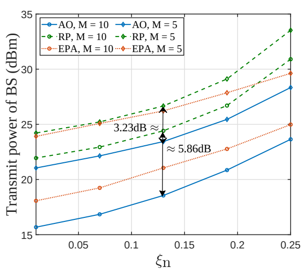

Fig. 3. Transmit power of BS versus the normalized channel estimation error with $N_t = 8$, $N_e = 2$, $R_{Q_1} = 2$bps/Hz, $R_{Q_2} = 1$bps/Hz, and $R_M = 0.5$bps/Hz.

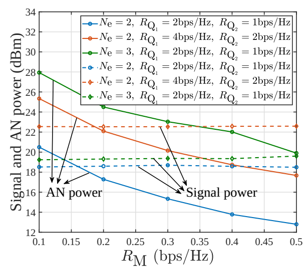

Fig. 4. Transmit power allocation between signals and AN versus the maximum eavesdropping rate at E with $N_t = 6$, $M = 10$, and $\xi_n = 0.1$.

and equal power allocation (EPA) (i.e., $|\mathbf{w}_1|^2 = |\mathbf{w}_2|^2$). As shown in Fig. 3, the total transmit power of three schemes monotonically decreases with the increased channel estimation error ξ_n, due to the fact that more transmit power is needed to compensate the increased channel uncertainty for secrecy guarantee. Compared with RP and EPA, the proposed AO algorithm achieves the lowest transmit power consumption. Particularly, the RP scheme has the worst performance and the performance gap between the RP scheme and the proposed AO algorithm increases from 3.23dB to 5.86dB when increasing M from 5 to 10. This is because that the random phase shifts cannot always strengthen that at legitimate users and/or suppress the received signals at E. Furthermore, by increasing the reflecting elements, the passive beamforming gain can be improved, which is helpful to the security enhancement.

In Fig. 4, the impact of the maximum eavesdropping rate on power allocation between signals and AN is plotted. As can be observed from Fig. 4, the maximum eavesdropping rate and the number of antennas at E have significant impact on the AN power rather than the signal power. This can be understood as follows. An increase in the eavesdropping rate reduces the security requirement of network, thus less AN power is needed. While an increase in the number of antennas will strengthen the interception ability of E, and thus, the BS should allocate more power to AN to suppress eavesdropping. Whereas both the maximum eavesdropping rate and the number of antennas at E have little impact on signal transmission. Furthermore, the QoS requirement of users has a great effect on both signal and AN power. This is due to the fact that an increase in the QoS constraint results in a higher transmit power, which in turns improves the received signal strength of E. Hence, more power are needed for AN to degrade the reception quality of E.

V. Conclusion

This letter proposed a robust beamforming scheme to enhance secrecy of the IRS assisted NOMA network against a multi-antenna eavesdropper. An efficient AO algorithm was developed to optimize transmit beamforming and IRS reflection coefficients for transmit power minimization. Numerical results were provided to validate the security effectiveness of the proposed scheme and obtain valuable design insights into the robust design of secure transmission via IRS.

References

[1] Q. Wu and R. Zhang, "Towards smart and reconfigurable environment: Intelligent reflecting surface aided wireless network," *IEEE Commun. Mag.*, vol. 58, no. 1, pp. 106–112, Jan. 2020.

[2] C. Huang, A. Zappone, G. C. Alexandropoulos, M. Debbah, and C. Yuen, "Reconfigurable intelligent surfaces for energy efficiency in wireless communication," *IEEE Trans. Wireless Commun.*, vol. 18, no. 8, pp. 4157–4170, Aug. 2019.

[3] Q. Wu and R. Zhang, "Intelligent reflecting surface enhanced wireless network via joint active and passive beamforming," *IEEE Trans. Wireless Commun.*, vol. 18, no. 11, pp. 5394–5409, Nov. 2019.

[4] L. Lv, J. Chen, Q. Ni, Z. Ding, and H. Jiang, "Cognitive non-orthogonal multiple access with cooperative relaying: A new wireless frontier for 5G spectrum sharing," *IEEE Commun. Mag.*, vol. 56, no. 4, pp. 188–195, Apr. 2018.

[5] L. Lv, H. Jiang, Z. Ding, L. Yang, and J. Chen, "Secrecy-enhancing design for cooperative downlink and uplink NOMA with an untrusted relay," *IEEE Trans. Commun.*, vol. 68, no. 3, pp. 1698–1715, Mar. 2020.

[6] B. Zheng, Q. Wu, and R. Zhang, "Intelligent reflecting surface-assisted multiple access with user pairing: NOMA or OMA?" *IEEE Commun. Lett.*, vol. 24, no. 4, pp. 753–757, Apr. 2020.

[7] X. Mu, Y. Liu, L. Guo, J. Lin, and N. Al-Dhahir, "Exploiting intelligent reflecting surfaces in NOMA networks: Joint beamforming optimization," *IEEE Trans. Wireless Commun.*, vol. 19, no. 10, pp. 6884–6898, Oct. 2020.

[8] Z. Ding and H. V. Poor, "A simple design of IRS-NOMA transmission," *IEEE Commun. Lett.*, vol. 24, no. 5, pp. 1119–1123, May. 2020.

[9] X. Guan, Q. Wu, and R. Zhang, "Intelligent reflecting surface assisted secrecy communication: Is artificial noise helpful or not?" *IEEE Wireless Commun. Lett.*, vol. 23, no. 9, pp. 1488–1492, Sept. 2019.

[10] H. Shen, W. Xu, S. Gong, Z. He, and C. Zhao, "Secrecy rate maximization for intelligent reflecting surface assisted multi-antenna communications," *IEEE Commun. Lett.*, vol. 23, no. 9, pp. 1488–1492, Sep. 2019.

[11] Z. Chu, W. Hao, P. Xiao, and J. Shi, "Intelligent reflecting surface aided multi-antenna secure transmission," *IEEE Wireless Commun. Lett.*, vol. 9, no. 1, pp. 108–112, Jan. 2020.

[12] X. Yu, D. Xu, Y. Sun, D. W. K. Ng, and R. Schober, "Robust and secure wireless communications via intelligent reflecting surfaces," *IEEE J. Sel. Areas Commun.*, vol. 38, no. 11, pp. 2637–2652, Nov. 2020.

[13] P. Cao, J. Thompson, and H. V. Poor, "A sequential constraint relaxation algorithm for rank-one constrained problems," in *Proc. 25th Eur. Signal Process. Conf. (EUSIPCO)*, Kosovo, 2017, pp. 1060–1064.

[14] L. Lv, Z. Ding, Q. Ni, and J. Chen, "Secure MISO-NOMA transmission with artificial noise," *IEEE Trans. Veh. Technol.*, vol. 67, no. 7, pp. 6700–6705, Jul. 2018.

[15] Z.-Q. Luo, J. F. Sturm, and S. Zhang, "Multivariate nonnegative quadratic mappings," *SIAM J. Optim.*, vol. 14, no. 4, pp. 1140–1162, Jul. 2004.

[16] B. Zheng, C. You, and R. Zhang, "Intelligent reflecting surface assisted multi-user OFDMA: Channel estimation and training design," *IEEE Trans. Wireless Commun.*, doi: 10.1109/TWC.2020.3021434.

[17] B. Zheng and R. Zhang, "Intelligent reflecting surface-enhanced OFDM: Channel estimation and reflection optimization," *IEEE Wireless Commun. Lett.*, vol. 9, no. 4, pp. 518-522, April 2020.

[18] Z. Luo, W. Ma, A. M. So, Y. Ye, and S. Zhang, "Semidefinite relaxation of quadratic optimization problems," *IEEE Signal Process. Mag.*, vol. 27, no. 3, pp. 20-34, May 2010.